Available online at www.sciencedirect.com
SCIENCE DIRECT®
Journal of Power Sources 137 (2004) 111–116
JOURNAL OF POWER SOURCES
www.elsevier.com/locate/jpowsour

Short communication

# Effects of surface modification by MgO on interfacial reactions of lithium cobalt oxide thin film electrode

Yasutoshi Iriyama*, Hiroyuki Kurita, Izumi Yamada, Takeshi Abe, Zempachi Ogumi

*Department of Energy and Hydrocarbon Chemistry, Graduate School of Engineering, Kyoto University, Katsura Campus, Nishigyo-ku, Kyoto 615-8510, Japan*

Received 6 February 2004; received in revised form 6 May 2004; accepted 24 May 2004
Available online 31 July 2004

**Abstract**

Magnesium oxide (MgO)-modified lithium cobalt oxide ($LiCoO_2$) thin film electrodes were prepared by pulsed laser deposition (PLD) and effects of surface modification by MgO on interfacial reactions of $LiCoO_2$ were studied. The modification by MgO was carried out by PLD on $LiCoO_2$ thin film electrode successively after the deposition of $LiCoO_2$ thin film by PLD. Auger electron spectroscopy suggested that Mg dispersed uniformly in *nano*-scale on the film electrode. Cyclic voltammetry measurements clearly showed that MgO modification suppresses the increase of resistances caused by repetition of lithium-ion insertion–extraction reaction charged up to 4.2 V versus $Li/Li^+$. Moreover, MgO modification decreased the activation energy of lithium-ion transfer reaction at $LiCoO_2$ thin film electrode–electrolyte interface, indicating that the modification by MgO affects the kinetics of lithium-ion transfer reaction at $LiCoO_2$–electrolyte interface.


*Keywords:* $LiCoO_2$ thin film electrode; Surface modification; Pulsed laser deposition; Lithium ion transfer; Li-ion batteries

## 1. Introduction

Lithium-ion batteries have been used as a power source of portable devices, such as cellular phones, notebook computers, etc. and, in recent years, they have been expected as a power source for hybrid vehicles (HEV), which will lead to the drastic decrease of fuel consumption. However, there are some problems to be solved for realization of advanced HEV, e.g. in- and out-put power densities, volumetric and gravimetric energy densities, cost, reliability, safety, and battery management systems.

Fast charge and discharge reactions are required for a practical use of lithium-ion batteries in HEV. For the fast charge and discharge reaction of lithium-ion batteries, the increase of lithium-ion transfer rate between the positive and negative electrode is indispensable. Employment of fine particles of electrode active materials is a practical way to enhance the transfer rate. Compared to large-size particles, diffusion path of lithium can be shortened in the fine particles, leading to the decrease of the resistance due to lithium diffusion in the electrode material. Moreover, fine particles have larger specific surface area. Consequently, the resistances due to charge transfer reaction can be decreased. Specific surface area of the active material increases with decreasing the size of an active material. Therefore, interfacial reactions (charge transfer reaction, electrolyte decomposition on the electrode material, etc.) should play much more important roles for lithium-ion batteries employing fine particles of active materials.

Lithium cobalt oxide ($LiCoO_2$) is one of the positive electrode material most widely used in lithium-ion batteries. Although theoretical capacity of $LiCoO_2$ ($0 < x < 1$ in $Li_xCoO_2$) is calculated to be about 280 mAh $g^{-1}$, only about a half of the capacity have been utilized in commercial lithium-ion batteries because of large capacity fading after extended cycling when lithium ions are extracted over this composition (about at 4.2 V versus $Li/Li^+$). In recent years, it has been reported that surface modification of $LiCoO_2$ by $ZrO_2$, $Al_2O_3$, MgO, DLC, etc. can suppress this large capacity fading and give excellent capacity retention even when cycled over 4.2 V versus $Li/Li^+$ [1–6]. However, effects of the surface modifications on interfacial reaction of $LiCoO_2$ electrode have not been clearly understood.

One of the methods to study interfacial reactions precisely on the above modified electrode materials is the use of their composite thin film electrodes. We have already prepared different kinds of positive electrode thin films,

* Corresponding author. Tel.: +81 75 383 2485; fax; +81 75 383 2488.
*E-mail address:* iriyama@elech.kuic.kyoto-u.ac.jp (Y. Iriyama).

0378-7753/$ – see front matter © 2004 Elsevier B.V. All rights reserved.
doi:10.1016/j.jpowsour.2004.05.029

including $LiCoO_2$, by pulsed laser deposition (PLD) and studied their electrochemical properties, especially focusing on the electrode–electrolyte interfacial reactions [7–9].

In this work, we prepared MgO-modified $LiCoO_2$ thin film electrodes by PLD and studied effects of surface modification by MgO on interfacial reactions of $LiCoO_2$ thin film electrode.

## 2. Experimental

Table 1 summarizes deposition conditions for preparing $LiCoO_2$ thin films by PLD. After depositing $LiCoO_2$ thin film on Pt substrate at 973 K for 1 h, MgO was deposited on $LiCoO_2$ thin film for 350 s successively at the same temperature. Hereafter the bare $LiCoO_2$ and MgO-modified $LiCoO_2$ thin films are referred to B-$LiCoO_2$ and Mg-$LiCoO_2$, respectively.

Prepared films were characterized by X-ray diffraction (XRD), Auger electron spectroscopy (AES), and X-ray photoelectron spectroscopy (XPS). Measurements by XRD were made using a Rigaku Rint 2500 diffractometer equipped with a Cu Kα radiation. Surface analysis of the film by AES was carried out using a Jeol JAMP-7800 F with field emission filament. Data of AES were collected from the area ranging from 15 nm to 10 μm in diameter. The chemical bond of the surface layer was also measured by XPS (ULVAC-PHI Model 5500, Mg source).

Electrochemical properties of the film electrode were studied using three-electrode cells. The working electrode was the film electrode deposited on Pt. Apparent surface area of the working electrode was 0.07 $cm^2$. The reference and counter electrodes were lithium metal. Hereafter, potentials described in this article are referred to $Li/Li^+$. The electrolyte solution was 1 mol $dm^{-3}$ $LiClO_4$ dissolved in propylene carbonate with water content <15 ppm (Kishida Chemical Co., Battery Grade). Electrochemical behaviors of the film electrode were examined by cyclic voltammetry (CV) and ac impedance spectroscopy. Cyclic voltammograms were obtained between 3.4 and 4.0 or 4.2 V at a potential sweep rate of 0.5 mV $s^{-1}$ using HOKUTO DENKO HSV-100. Impedance measurements were conducted using a Solartron 1260 frequency response analyzer coupled with a Solartron 1287 potentiostat. Thin film electrode was cycled once between 3.4 and 4.0 V in advance, and the electrode was scanned to 4.0 V at 1 mV $s^{-1}$ followed by keeping the potential for 2 h to attain steady state. The impedance at 4.0 V was measured by applying a sine wave of 5 mV (rms) amplitude over the frequency range of 10 kHz to 10 mHz. This measurement was conducted every 10 K over the temperature range from 278 to 313 K.

Table 1
Preparation conditions for $LiCoO_2$ thin films and the surface modification by MgO

| | |
|---|---|
| Laser (KrF Excimer laser) (nm) | 248 |
| Repetition frequency (pps) | 10 |
| Laser fluence (J $cm^{-2}$) | 1.4 |
| Target-substrate distance (mm) | 50 |
| Substrate temperature (K) | 973 |
| Pressure ($O_2$) (Pa) | 26 |
| Deposition time for $LiCoO_2$ (h) | 1 |
| Deposition time for MgO (s) | 350 |

## 3. Results and discussions

### 3.1. Characterization of Mg-$LiCoO_2$

Fig. 1(a) shows an XRD pattern of the B-$LiCoO_2$ deposited on Pt for 1 h. Diffraction peaks at $2\theta = 18.95^\circ$ was indexed as the 003 reflection of hexagonal $LiCoO_2$. The other diffraction lines marked by * were derived from the substrate or adhesive tapes. As shown in this pattern, no reflection line such as 1 0 1, 0 1 2, and 1 0 4, which are usually observed in $LiCoO_2$ powder samples, appeared, indicating that the film has a preferred *c*-axis orientation [11,12]. Fig. 1(b) shows an XRD pattern of the Mg-$LiCoO_2$. Peak shift of 0 0 3 reflection was not observed before and after the surface modification by MgO within the detectable limit of XRD. Diffraction peaks derived from MgO are not observed in this pattern of Fig. 1(b). This is due to the very small quantity of MgO in the Mg-$LiCoO_2$ surface.

The distribution of Mg in the Mg-$LiCoO_2$ surface was examined by AES. Fig. 2 shows AES spectra of the Mg-$LiCoO_2$. Measurement area of Fig. 2(a) and (b) was 10 μm and 15 nm in diameter, respectively. In both spectra, Auger peaks indexed as O KLL (two peaks), Co LMM (three peaks), and Mg KLL (one peak) were observed at around 500, 700, and 1180 eV, respectively. As shown in

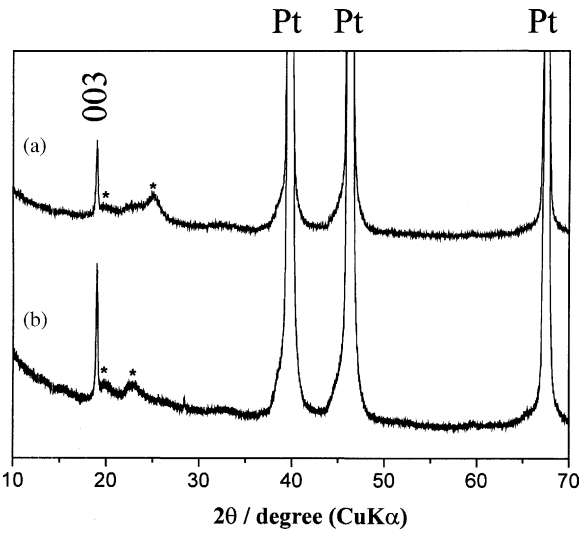


Fig. 1. XRD patterns of: (a) a bare and (b) an MgO-modified $LiCoO_2$ thin film electrodes deposited on Pt substrates. Peaks marked by * originate from substrate holder or adhesive tapes.

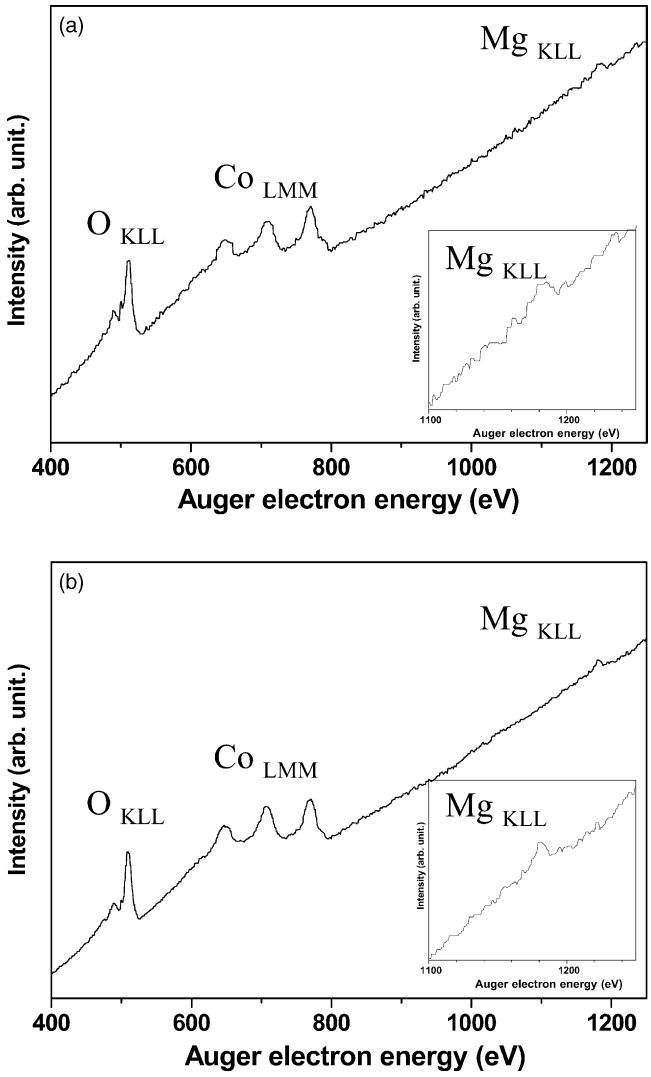


Fig. 2. AES spectra on an MgO-modified $LiCoO_2$ thin film electrode surface. The measurement area is: (a)10 μm and (b) 15 nm in diameter. Insets shown in both spectra are magnified spectrum around Mg KLL peak.

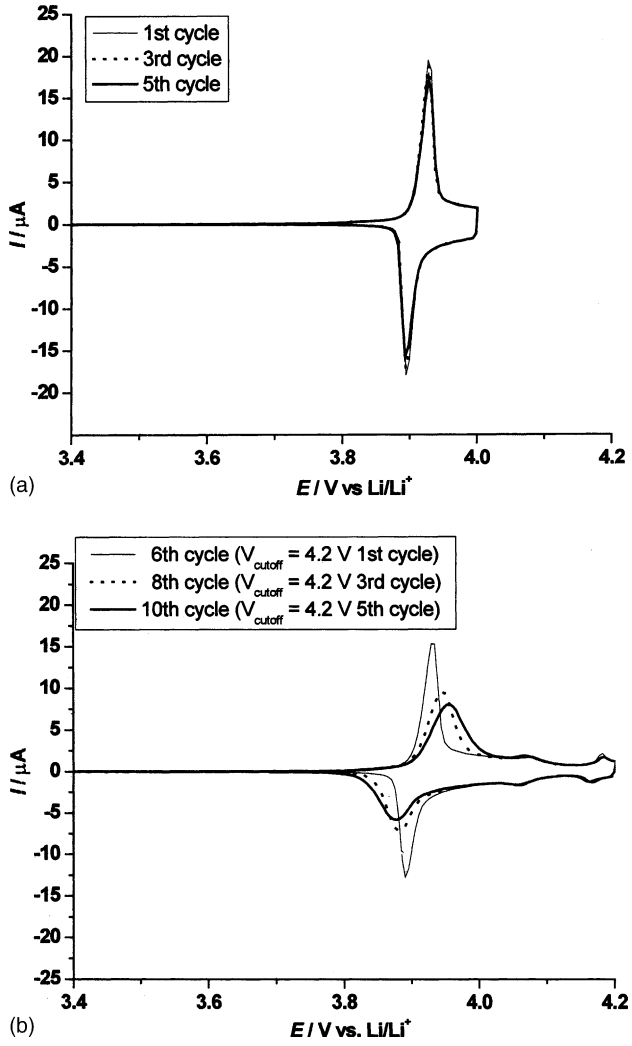


Fig. 3. Cyclic voltammograms of a bare $LiCoO_2$ thin film electrode. (a) CVs were repeated for five times between 3.4 and 4.0 V. (b) CVs were repeated for five times between 3.4 and 4.2 V after the CVs shown in Fig. 3(a). $v = 0.5\,mV\,s^{-1}$.

Fig. 2(a), both Co LMM and Mg KLL peaks are clearly observed in the area of 15 nm in diameter. We carried out same measurement at several points on the film electrode and found Auger peaks indexed as O KLL, Co LMM, and Mg KLL in all spectra. Generally, Auger electrons penetrate only a few atomic layers (about 1 nm in this energy area) of solid. Hence, these results strongly suggest that Mg disperses in nano-scale in the Mg-$LiCoO_2$ surface. Moreover, peak intensity ratios of each spectrum did not depend on its measurement area as shown in Fig. 2, indicating that Mg dispersed quite uniformly in the Mg-$LiCoO_2$ surface.

We measured the XPS spectra in both the B-$LiCoO_2$ and Mg-$LiCoO_2$ surface and found that there was no change of Co 2p spectra before and after the MgO modification. Tsukamoto et al. have studied the electronic conductivity of Mg-doped $LiCoO_2$ and suggested that the Mg doping will increase or decrease the volume of $Co^{3+}$ in $LiCoO_2$ for the charge compensation [13]. Hence, no change of Co2p XPS spectrum means that this MgO modification did not form solid solutions in the $LiCoO_2$ electrode surface.

### 3.2. Effects of the surface modification by MgO on the stability of electrode reaction

Figs. 3 and 4 show cutoff voltage dependency of CVs for the B-$LiCoO_2$ and Mg-$LiCoO_2$, respectively, at 303 K. Potential sweep rate of all voltammograms was $0.5\,mV\,s^{-1}$. These CVs were measured between the initial (3.4 V) and cut off voltages (= $V_{cutoff}$; $V_{cutoff}$ = 4.0 or 4.2 V). In case of $V_{cutoff}$ = 4.0 V, anodic and cathodic current peaks were observed at around 3.9 V given by Figs. 3(a) and 4(a). The redox couple at 3.9 V is attributed to a first-order phase transition of $LiCoO_2$ [11,12]. When CVs were repeated in this potential region (below the potential of 4.0 V) for five times, voltammograms remained unchanged even after fifth cycle

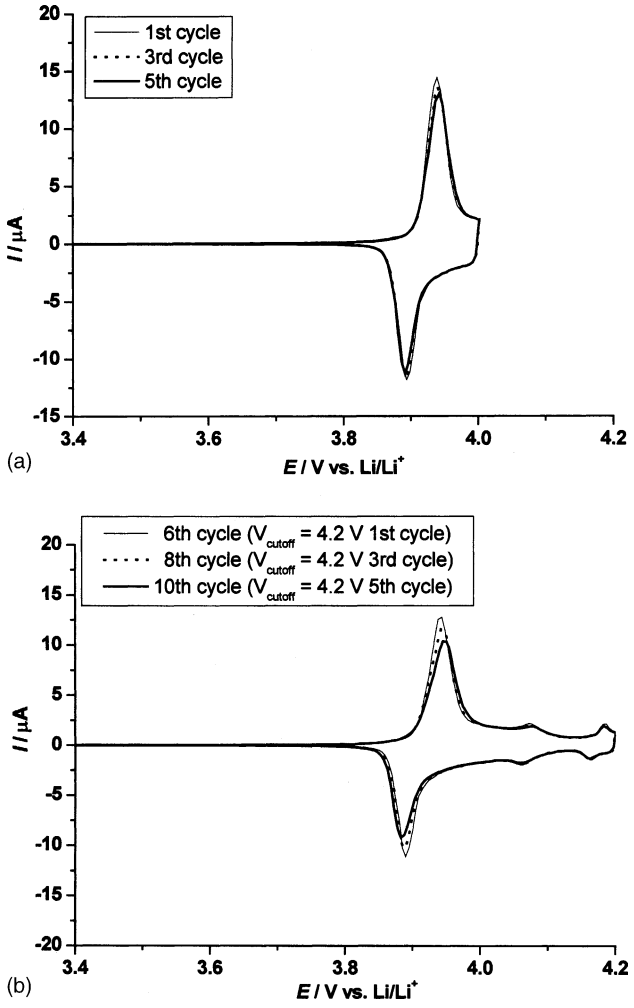


Fig. 4. Cyclic voltammograms of an MgO-modified $LiCoO_2$ thin film electrode. (a) CVs were repeated for five times between 3.4 and 4.0 V. (b) CVs were repeated for five times between 3.4 and 4.2 V after the CVs shown in Fig. 4(a). $v = 0.5\,mV\,s^{-1}$.

as shown in Figs. 3(a) and 4 (a). When the $V_{cutoff}$ increased up to 4.2 V, two couples of redox peaks at around 4.08 and 4.15 V were newly observed. These two peaks are ascribed to the phase transition of $LiCoO_2$ between the hexagonal and monoclinic phase [11,12]. When CVs were repeated in this potential region (below the potential of 4.2 V) for 5 times, the first-order phase transition peak of the B-$LiCoO_2$ became broader and both the anodic and cathodic peak potentials shifted to the potential sweep direction with the increment of cycles as shown in Fig. 3(b). On the other hand, peak shift and broadening of the first-order phase transition peak at around 3.9 V were not clearly observed in CVs of the Mg-$LiCoO_2$ given in Fig. 4(b).

Table 2 summarizes the variations of the peak separation potential ($\Delta E_p$ (mV)) of the first-order phase transition peak and the relative charging capacity with the cycles. Here, the charging capacity was evaluated by integrating the anodic current in Fig. 3(a) and (b) and Fig. 4(a) and (b), and the relative charging capacity was calculated by dividing each charging capacity by the initial charging capacity. In case of $V_{cutoff} = 4.0$ V, $\Delta E_p$ of both electrodes increased only a few mV even after fifth cycle. Values of $\Delta E_p$ of the Mg-$LiCoO_2$ were about 10 mV larger than those of the B-$LiCoO_2$ through five cycles, which will be explained later. In case of $V_{cutoff} = 4.2$ V, the value of $\Delta E_p$ of the Mg-$LiCoO_2$ at fifth cycle increased by only 6 mV compared to the first cycle at $V_{cutoff} = 4.2$ V, while difference of $\Delta E_p$ of the B-$LiCoO_2$ between the first and fifth cycle was 37 mV. This result clearly reveals that the surface modification by MgO on $LiCoO_2$ thin film electrode suppresses the increase of resistance caused by repetitions of the electrochemical lithium-ion insertion–extraction reaction charged up to 4.2 V. Although the cycle was not repeated enough in both cutoff voltages, the relative charging capacity ratio after the 5th cycle was slightly improved by MgO modification. This tendency was in good agreement with previous works [4,5].

Wang et al. have prepared amorphous MgO-coated $LiCoO_2$ powder and reported that these modifications improved the cycle ability of $LiCoO_2$ charged over 4.3 V [4]. They attributed the improved capacity retention by MgO coating to the protection of the active material from the acidic electrolyte, resulting in the prevention of the dissolution of the $Co^{4+}$ ions. Mladenov et al. studied the electrochemical properties of MgO-coated $LiCoO_2$ and reported that the MgO coating contributes to the particle integrity of $LiCoO_2$, which is destroyed by cobalt dissolution and/or the mechanical failure of the active material [5]. In contrast to the above reports, Amatucci et al. reported that

Table 2
Variations of relative charging capacities and peak separation potential of the first-order phase transition peak ($\Delta E_p$) with the cycles vs. cutoff voltages

| At 4.0 V | | 1st | 2nd | 3rd | 4th | 5th |
|---|---|---|---|---|---|---|
| Bare $LiCoO_2$ | Relative capacity | 1.00 | 0.97 | 0.95 | 0.95 | 0.94 |
| | $\Delta E_p$ (mV) | 34 | 34 | 35 | 34 | 37 |
| MgO-modified $LiCoO_2$ | Relative capacity | 1.00 | 0.98 | 0.96 | 0.95 | 0.95 |
| | $\Delta E_p$ (mV) | 44 | 42 | 47 | 48 | 49 |
| Bare $LiCoO_2$ | Relative capacity | 1.00 | 0.96 | 0.95 | 0.93 | 0.93 |
| | $\Delta E_p$ (mV) | 40 | 45 | 55 | 62 | 77 |
| MgO-modified $LiCoO_2$ | Relative capacity | 1.00 | 0.97 | 0.97 | 0.95 | 0.95 |
| | $\Delta E_p$ (mV) | 56 | 56 | 55 | 61 | 62 |

cobalt dissolution from $LiCoO_2$ is not likely to occur at the potential less than 4.2 V [10]. Therefore, the dissolution of $Co^{4+}$ ions cannot be responsible for the increase of $\Delta E_p$ with the cycles charged up to 4.2 V. Phase transition peaks of $LiCoO_2$ between the hexagonal and monoclinic phase are clearly observed at around 4.08 and 4.15 V in both spectra of Figs. 3(b) and (b). Hence, the improvements of electrochemical properties by MgO modification as given in Fig. 4(b) are not also due to the suppression of the phase transition in the film electrode.

From the above considerations, one of the probable explanations of the enhancement of electrochemical properties is the structural stability around the electrode surface by the surface modification. The effective ionic radius of $Mg^{2+}$ with a coordination number of 6 is about 86 pm, which is almost the same with that of $Li^+$ (90 pm), and therefore $Mg^{2+}$ migration from some of MgO into $LiO_2$-layers is quite likely to take place [4]. The migration of $Mg^{2+}$ into a $LiO_2$-layer will increase the attraction of adjacent $CoO_2$-layers due to its higher valance. This strong attraction will stabilize layered structure around $LiCoO_2$surface, resulting in the suppression. In fact, AES analysis revealed that Mg disappeared from the Mg-$LiCoO_2$ surface after extended cycling.

### 3.3. Effects of the surface modification by MgO on the charge transfer reaction of $LiCoO_2$ thin films

Both B-$LiCoO_2$ and Mg-$LiCoO_2$ exhibited stable lithium-ion insertion–extraction reaction below 4.0 V as shown in Figs. 3(a) and 4(a). Hence, we next studied charge transfer resistances at 4.0 V by AC impedance measurement. Fig. 5 shows AC impedance spectra of both the B-$LiCoO_2$ and Mg-$LiCoO_2$ at 4.0 V obtained at 303 K. Each spectrum consisted of a semicircle in the high frequency region (>20 Hz), which is assigned to the charge

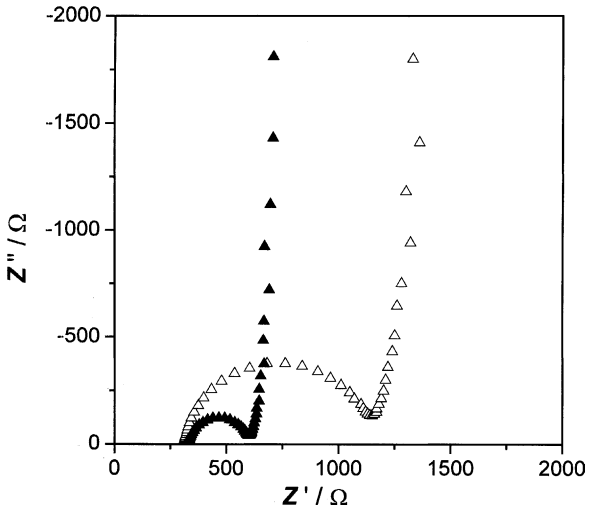


Fig. 5. The ac impedance spectra of both a bare (closed triangles) and an MgO-modified $LiCoO_2$ (open triangles) thin film electrodes at 4.0 V.

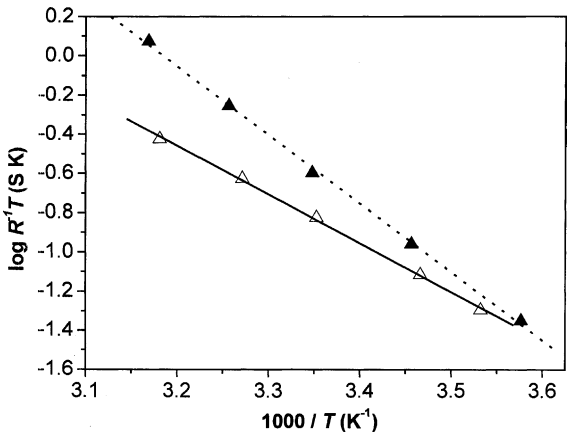


Fig. 6. Temperature dependency of charge transfer resistances of a bare (closed triangles) and an MgO-modified (open triangles) $LiCoO_2$ thin film electrodes at 4.0 V.

transfer resistance, followed by a straight line with a nearly vertical line in the lower frequency region (<20 Hz), corresponding to finite-space diffusion. The charge transfer resistances of both the B-$LiCoO_2$ and Mg-$LiCoO_2$ were evaluated from the spectra to be 250 and 750 Ω, respectively. An electrochemically inactive layer, including MgO, formed on the Mg-$LiCoO_2$ surface, probably causes the larger charge transfer resistance of the Mg-$LiCoO_2$. The larger $\Delta E_p$ of the Mg-$LiCoO_2$ compared to that of the B-$LiCoO_2$ as shown in Table 2 is principally due to this larger charge transfer resistance of the Mg-$LiCoO_2$ at 303 K.

Temperature dependency of the charge transfer resistances of both electrodes was elucidated. The Arrhenius plots of reciprocal charge transfer resistance multiplied by absolute temperature against reciprocal temperature are shown in Fig. 6. The open and solid triangles denote the B-$LiCoO_2$ and Mg-$LiCoO_2$, respectively. As shown in Fig. 6, these plots can be fitted by a straight line. Although, in the temperature range studied in this work, charge transfer resistances of the Mg-$LiCoO_2$ were larger than those of the B-$LiCoO_2$, we can expect from Fig. 6 that the charge transfer resistance of the Mg-$LiCoO_2$ become smaller than that of the B-$LiCoO_2$ at lower temperatures (under 278 K). Activation energy of the charge transfer reaction of the Mg-$LiCoO_2$ was calculated from the slope to be 0.49 eV, which was smaller than that of the B-$LiCoO_2$, 0.64 eV.

Raistrick has studied the temperature dependency of electrochemical lithium insertion–extraction reaction of $Na_{0.64}WO_3$ and reported that charge transfer reaction of $Li_xNa_{0.64}WO_3$ have single activation energy and that it is independent of potential, that is, electron concentration in $Li_xNa_{0.64}WO_3$ [14]. From these results, he suggested that the rate determining step of this charge transfer reaction is associated with the ion transfer rather than the electron transfer. The electron conductivity of $Na_{0.64}WO_3$ has been reported to be ca. $5 \times 10^3$ S cm$^{-1}$ [15]. On the other hand, the electron conductivity of $Li_{0.60}CoO_2$ that is expected

composition at 4.0 V has been reported to be ca. $1 \times 10^1$ S cm$^{-1}$ [16]and the thickness of the $LiCoO_2$ films was quite thin (ca. 0.1 μm). Because we can expect that both $LiCoO_2$ films at 4.0 V and $Na_{0.64}WO_3$ obtain quite high electron conductivities compared to ionic conductivities, it is reasonable to expect that the rate determining step of charge transfer reaction of $LiCoO_2$ is also associated with the ion transfer reaction. Hence, the decrease of the activation energy for the charge transfer reaction is probably caused by some interactions between modification oxides and lithium-ions. Quite recently, we found that $ZrO_2$ modification could decrease the activation energy but the effect was small compared with MgO modification. If the decrease of the activation energy was only due to the prevention of some side reactions, the activation energy will obtain a same value in both cases. Although precise mechanism cannot be clarified only in this work, it should be noted that surface modification techniques affect not only the stabilization of electrode reactions but also the kinetics of charge transfer reaction.

## 4. Conclusions

Surface modification by MgO on $LiCoO_2$ thin film electrode is effective to suppress the increase of the resistance caused by repetition of lithium-ion insertion–extraction reaction of $LiCoO_2$ charged up to 4.2 V versus Li/Li$^+$. This should be due to the stabilization of the layered-structure around the electrode surface brought by $Mg^{2+}$ migration into $Li_2O$-layers. It is very interesting that MgO modification decreases the activation energy of interfacial lithium ion-transfer reaction at $LiCoO_2$ thin film electrode–electrolyte. These results revealed that the surface modification by MgO on $LiCoO_2$ thin film electrode was effective to improve the kinetics of lithium-ion transfer reaction at electrode–electrolyte interface.

## Acknowledgements

This work was supported by CREST of JSTA (Japan Science and Technology Agency), by New Energy and Industrial Technology Development Organization (NEDO) of Japan, and also by a Grant-in-Aid for 21st COE program-COE for a United Approach to New Materials Science- from the Ministry of Education, Culture, Sports, Science, and Technology.

## References

[1] J. Cho, Y.J. Kim, T.-J. Kim, B. Park, Angew. Chem. Int. Ed. 40 (2001) 3367.
[2] J. Cho, C.-S. Kim, S.-I. Yoo, Electrochem. Solid State Lett. 3 (2000) 362.
[3] Y.J. Kim, T.-J. Kim, J.W. Shin, B. Park, J. Cho, J. Electrochem. Soc. 149 (2002) 1337.
[4] Z. Wang, C. Wu, L. Liu, F. Wu, L. Chen, X. Huang, J. Electrochem. Soc. 149 (2002) 466.
[5] M. Mladenov, R. Stoyanova, E. Zhecheva, S. Vassilev, Electrochem. Commun. 3 (2001) 410.
[6] E. Endo, T. Yasuda, A. Kita, K. Yamaura, K. Sekai, J. Electrochem. Soc. 147 (2000) 1291.
[7] M. Inaba, T. Doi, Y. Iriyama, T. Abe, Z. Ogumi, J. Power Sources 81–82 (1999) 554.
[8] Y. Iriyama, M. Inaba, T. Abe, Z. Ogumi, Solid State Ion. 135 (2000) 95.
[9] Y. Iriyama, M. Inaba, T. Abe, Z. Ogumi, J. Power Sources 94 (2001) 175.
[10] G.G. Amatucci, J.M. Tarascon, L.C. Klein, Sold State Ion. 83 (1996) 167.
[11] J.N. Reimers, J.R. Dahn, J. Electrochem. Soc. 139 (1992) 2091.
[12] G.G. Amatucci, J.M. Tarascon, L.C. Klein, J. Electrochem. Soc. 143 (1996) 1114.
[13] H. Tukamoto, A.R. West, J. Electrochem. Soc. 144 (1997) 3164.
[14] I.D. Raistrick, Solid State Ion. 9/10 (1983) 425.
[15] P.A. Lightsey, D.A. Lilienfeld, D.F. Holcomb, Phys. Rev. B 14 (1976) 4730.
[16] M. Ménétrier, I. Saadoune, S. Levasseur, C. Delmas, J. Mat. Chem. 9 (1999) 1135.